Influence of inlaid material, yarn and knitted structure on the net buoyant force and mechanical properties of inlaid knitted fabric for buoyant swimwear

Abstract

Buoyant swimwear is becoming more common in recreational swimming use so the performance of buoyant fabric is important when designing functional swimwear. In this study, potential buoyant inlaid knitted fabrics for buoyant swimwear are investigated. Three types of knitted structures, half milano, full milano and 1x1 rib, are selected and various kinds of tubes and foam rods in different diameters are prepared for inlaying during the knitting process by using a 7G hand-knitting machine. The mean differences among the levels of three independent variables: (1) inlaid material, (2) yarn and (3) knitted structure on three dependent variables (net buoyant force, compression, and tensile properties) are analysed by using MANOVA. The result shows that the net buoyant force and mechanical properties of the fabric are significantly different due to the inlaid material and knitted structure, but not the yarn. The net buoyant force increases with fabric thickness and the outer diameter of the inlaid material. The inlaid fabrics are less compressible than the control fabric and show better recoverability with

an increase in the diameter of the inlaid material. For the tensile properties, the inlaid material reinforces the fabric in both the wale and course directions in which the stiffness in the course direction is significantly increased. The inlaid fabric is stronger and resistant to breakage in the course direction when the diameter of the inlaid material is increased. The findings of this study contribute to developments in the textile and sportswear industry.

Keywords

buoyancy, compression, tensile, inlay knitting, knitted structure

Introduction

Buoyant swimwear has gained popularity in the global market[1] and is recommended for beginners because it can reduce risk and instil more confidence in swimmers.[2-4] Its use also changes the swimming teaching-learning process.[5] Air and foam are common buoyant media used in swimwear due to their low density[6] and flexibility.[7] Neoprene, expanded polystyrene, polyurethane foam, ethylene vinyl acetate foam, polyethylene (PE) and polyvinyl chloride (PVC) foam are common buoyant media used in swimwear.[4, 7-12] However, these materials have various drawbacks. Air chambers are susceptible to puncture, which can be dangerous as buoyancy can be lost.[8] Unbalanced

buoyant foam blocks can be cumbersome for the wearers when they attempt to swim horizontally[7] and extremely bulky due to the uneven distribution of buoyancy in other areas.[13] Thus, the construction and effects of buoyant materials have been investigated by researchers to address the safety and aesthetic needs of customers and the industry.

The development of buoyant fabric with air containers or foam rods has been investigated in several studies.[14-17] The thickness and structure of knitted fabric have been found to have a significant effect on the weight, tensile, moisture management and compression properties of the fabric.[18-22] The focus of this study is therefore the effect of inlaid material, yarn and knitted structure on the net buoyant force and the compression and tensile properties of buoyant fabric. Polypropylene (PP) fibres are used extensively in commercial swimwear and sportswear[23, 24] and PP hollow fibre has been used to create buoyant layers for filtration[25, 26] due to its low density and ability to trap air between the fibres.[27] To maximise swimwear buoyancy, other types of buoyant materials such as tubes and foam rods can be used in addition to polypropylene fabric. Polyvinyl chloride (PVC) has been used for flexible medical tubing.[28] It is soft and flexible and thus has potential as buoyant tubes. Silicone is widely used in tissue engineering due to its high chemical inertness and good mechanical properties,[29] and polyethylene (PE) foam is prevalent in buoyant swimwear and pool toys[30-32] due to its buoyant properties.[30]

3

Inlaid knitting can enable the coarse buoyant materials to be fabricated using a knitting machine, as the inlaid materials that cannot be knitted as part of the loops of the ground structure can be securely incorporated into the fabric.[33] The yarn is initially locked inside the loop and prevented from being hooked on to the knitting needles when the carrier supplies the knitting yarn, and inlay knitting can then be conducted.[34, 35] The yarn can be laid-in easily in a rib arrangement [36] and also in other forms of double knitted structure in knitted fabric because of the space created between the loops situated on the front and back needle beds. Double knitted structure, including half milano, full milano and 1x1 rib, can therefore be used. The half milano structure consists of one row of double jersey and one row of single jersey; the full milano consists of a row of single jersey on the front and back needle beds and a row of double jersey; and the 1x1 rib structure consists of one row of double jersey.[37, 38] Advances in knitting technology have led inlaid knitted fabric structures to be used in structural design, household applications and industrial applications.[36, 39-43] They have also been applied in compression garments for healthcare and medical uses.[44-47]

Although the application of inlaid knitted fabric has been examined in some studies, little research has been done on the relationship between the inlaid material, yarn and knitted structure and buoyancy performance, or the mechanical properties of inlaid knitted buoyant fabric. In this study, the effects of the inlaid material, yarn and

knitted structure on the net buoyant force, compression and tensile properties of inlaid knitted fabrics are investigated. To facilitate an efficient data collection process, a design of experiments (DOE) table was used (Table 1). The findings of this study provide a better understanding of the effects that the inlaid knitted structure has on the properties of buoyant fabric, which affects the fabric selection criteria when developing buoyant swimwear. The results of this study are of benefit to the textile and sportswear industries.

Table 1. Design of experiment (DOE)

Factor	Levels				
Inlaid material	Polyvinyl chloride (PVC) tube	Silicone tube	Polyethylene (PE) tube	Expandable polyethylene (EPE) foam rod	Silicone foam rod
Yarn	Solid polypropylene	Hollow polypropylene			
Knitted structure	1x1 rib	Half milano	Full milano		

Materials

Knitting materials

Three tubes and two foam rods of various diameters were sourced from the market. PE, PVC and silicone were chosen as they are buoyant, flexible and soft enough to be laid-in during the knitting process. The details and cross-sections of each inlaid tube, the foam rods and the knitting yarn are provided in Table 2 and illustrated in Figure 1. Due to the advantages of the space created with double knitted structure, half milano, full milano and 1x1 rib were selected as the main structures of the knitted fabric for comparison. The configuration of the three knitted structure were simulated using the SDS-ONE Apex software (SHIMA SEIKI MFG., LTD., Japan), as shown in Figure 2. The notations and specification of the three types of double knitted structure are given in Tables 3 and 4.

Preparation of the buoyant inlaid knitted fabric

Twenty-five buoyant fabric samples consisting of different inlaid materials, yarns and knitted structure were fabricated, and four knitted fabric samples without inlays in three knitted structures were taken as the controls. The fabric samples were knitted on a V-bed hand-knitting machine (Wealmart Asia Limited, China), in which the gap between the two needle beds was adjusted from 4.5 mm to 8 mm for laying-in the buoyant

material. The machine gauge of the V-bed hand-knitting machine (the number of needles per inch) was 7. The weight determining the take-down tension during knitting was pre-set at 364.55 g. The inlaid fabric was knitted using three ends of 75D/72F 100% solid polypropylene or one end of 250D hollow polypropylene yarn as the knitting yarn and one end of the tube/rod as the inlaid material. All of the samples were prepared under the same knitting tension and parameters, with a dimension of 38 courses that included 25 inlays and 40 wales. The lengths of the inlaid tube and foam rod were set to 337.56 cm with a 2% variation. Both ends of the inlaid tube were blocked by heat fusion. Five replicates were taken for each knitting condition. The details of the sample specifications are given in Table 5 and the inlaid knitted fabrics EPEnH2 and EPE2 are illustrated in Figure 3.

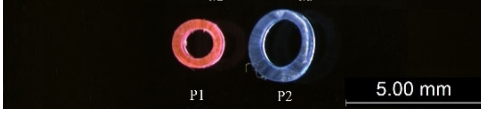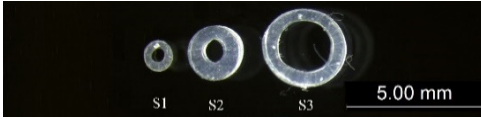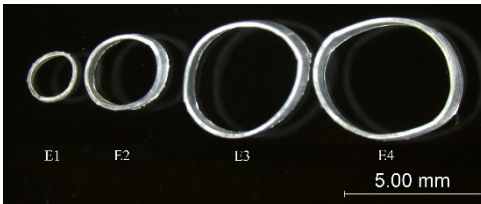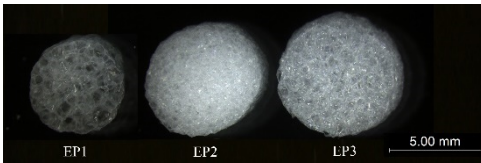**Table 2.** Materials used for the inlay and knitted parts
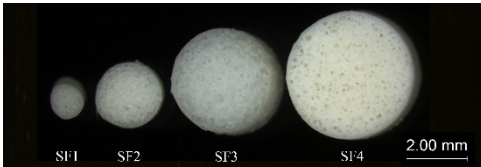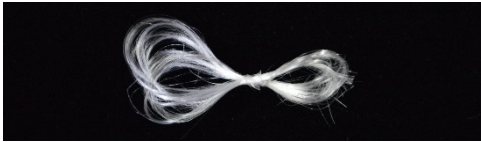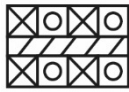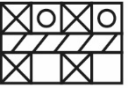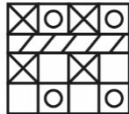
Inlaid material/ knitting yarn	Code	Material	Microscopic view/image
Inlaid tube	P1-P2	Polyvinyl chloride (PVC)	
	S1-S3	Silicone	
	E1-E4	Polyethylene (PE)	
Inlaid foam	EP1-EP3	Expandable polyethylene (EPE)	
	SF1-SF4	Silicone foam	
Yarn	PP	75D/72F 100% solid polypropylene (PP)	
	HPP	250D 100% hollow polypropylene (HPP)	

Table 3. Notation and specifications of three types of knitted structures

Structure	Notation diagram	Type of stitch	Number of loops	
			Front needle bed	Back needle bed
1 × 1 rib		All knit stitches	1	1
Half milano		Knit and miss stitches	2	1
Full milano		Knit and miss stitches	2	2

⊠ Knit stitch (technical face)

◎ Knit stitch (technical back)

▢ Miss stitch
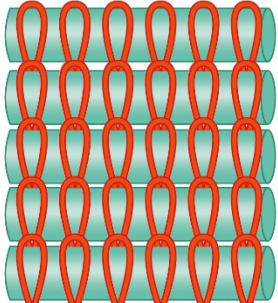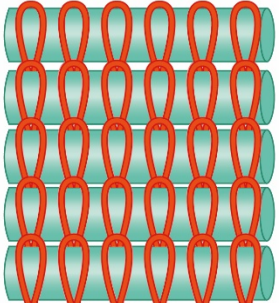
◩ Inlaid material

Table 4. Images of the three types of double knitted structures

Structure	Image of inlaid knitted fabric	
	Front view	Back view
1 × 1 rib		
Half milano		
Full milano		

Yarn ▬▬ Inlaid material ⬭

Table 5. Specifications of the buoyant inlaid knitted fabrics and the control fabrics

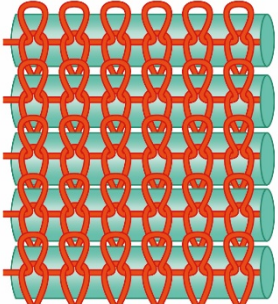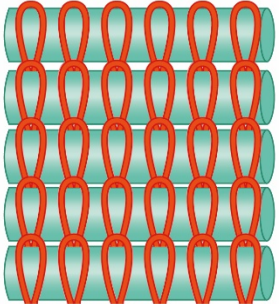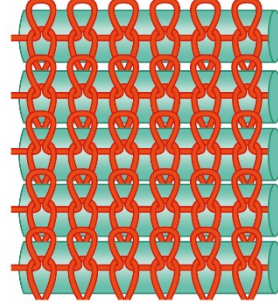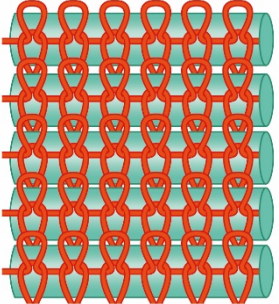| Fabric code	Inlaid material	Yarn	Knitted structure	Properties of the inlaid material			
				Inner Diameter (mm)	Outer Diameter (mm)	Linear Density (g/cm)	Wall Thickness of Tube (mm)
PV1	P1	PP	Half milano	1.17	1.86	0.020	0.70
PV2	P2	PP	Half milano	1.64	2.46	0.033	0.82
SI1	S1	PP	Half milano	0.56	1.09	0.008	0.54
SI2	S2	PP	Half milano	0.84	1.97	0.029	1.13
SI3	S3	PP	Half milano	1.95	2.84	0.043	0.88
PE1	E1	PP	Half milano	1.57	1.83	0.006	0.26
PE2	E2	PP	Half milano	2.52	2.83	0.018	0.31
PE3	E3	PP	Half milano	3.95	4.27	0.018	0.32
PE4	E4	PP	Half milano	4.48	4.82	0.037	0.35
EPE1	EP1	PP	Half milano	Nil	5.24	0.005	Nil
EPE2	EP2	PP	Half milano	Nil	6.11	0.006	Nil
EPE3	EP3	PP	Half milano	Nil	6.36	0.005	Nil
SIF1	SF1	PP	Half milano	Nil	1.15	0.008	Nil
SIF2	SF2	PP	Half milano	Nil	2.21	0.019	Nil
SIF3	SF3	PP	Half milano	Nil	3.31	0.063	Nil
SIF4	SF4	PP	Half milano	Nil	4.26	0.105	Nil
EPEm1	EP1	PP	Full milano	Nil	5.24	0.005	Nil
EPEm2	EP2	PP	Full milano	Nil	6.11	0.006	Nil
EPEm3	EP3	PP	Full milano	Nil	6.36	0.005	Nil
EPEn1	EP1	PP	1 x 1 rib	Nil	5.24	0.005	Nil
EPEn2	EP2	PP	1 x 1 rib	Nil	6.11	0.006	Nil
EPEn3	EP3	PP	1 x 1 rib	Nil	6.36	0.005	Nil
EPEnH1	EP1	HPP	1 x 1 rib	Nil	5.24	0.005	Nil
EPEnH2	EP2	HPP	1 x 1 rib	Nil	6.11	0.006	Nil
EPEnH3	EP3	HPP	1 x 1 rib	Nil	6.36	0.005	Nil
Ch	Nil	PP	Half milano	Nil	Nil	Nil	Nil
Cm	Nil	PP	Full milano	Nil	Nil	Nil	Nil
Cn	Nil	PP	1 x 1 rib	Nil	Nil	Nil	Nil
CnH	Nil	HPP	1 x 1 rib	Nil	Nil	Nil	Nil

PP: solid polypropylene; HPP: hollow polypropylene.
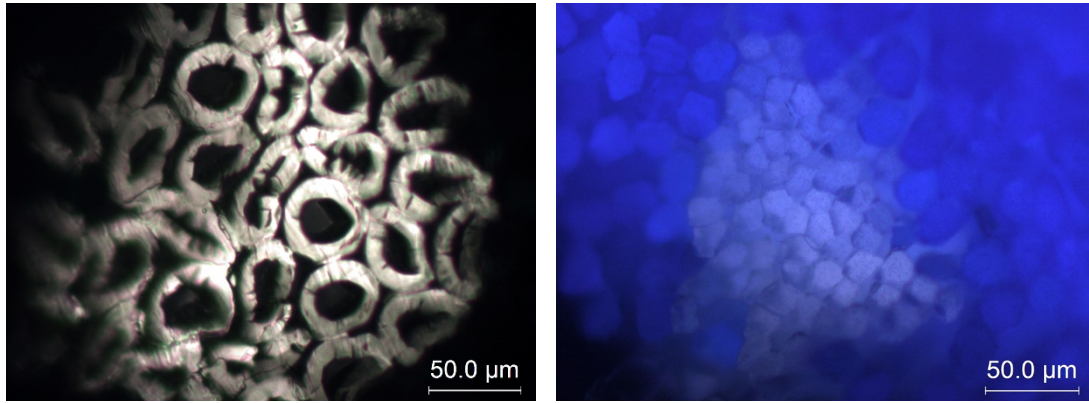
Figure 1. Scanning electron microscopy images of the cross-sections of (a) 250D hollow polypropylene yarn; (b) 75D/72F solid polypropylene yarn
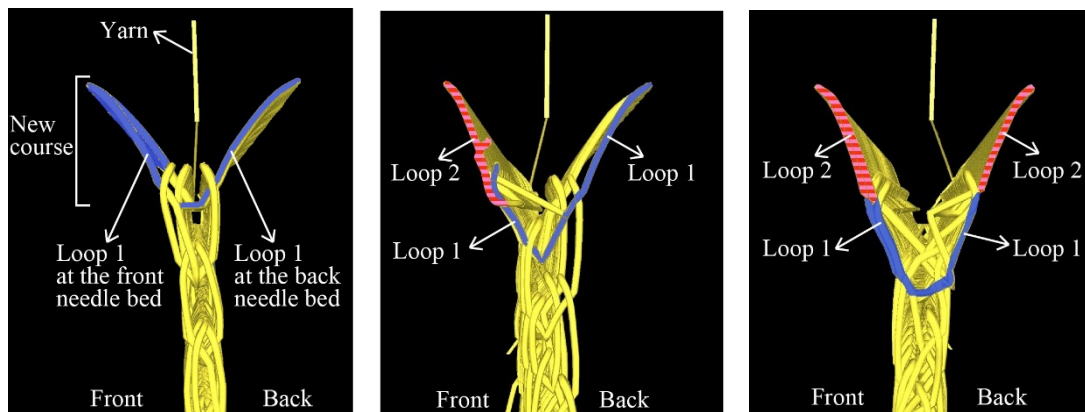
■ Loops in 1x1 rib structure

▨ Additional loop (compared with 1x1 rib)

Figure 2. Side view of knitted structure simulation of (a) 1x1 rib; (b) half milano and (c) full milano
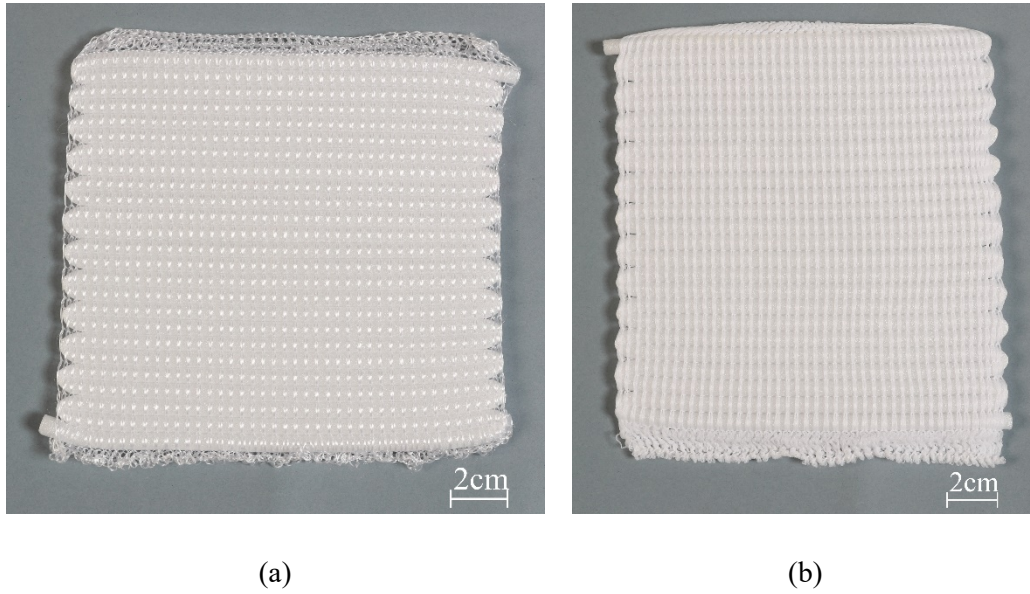
Figure 3. Front view of the inlaid knitted fabric (a) EPEnH2; (b) EPE2

Measurement

To examine the relationships among the inlaid material, yarn and knitted structure on the net buoyant force, the volume of the fabric was measured and the net buoyant force was calculated based on the Archimedes' principle. This method was validated by using buoyancy measurement systems with a good agreement between the calculated and measured buoyant forces.[48] As the buoyant tubes and foam rods used in this study are highly compressible, the inner and outer diameters of the tubes and the outer diameters of rods were measured in four directions with a stereo microscope (M165C, Leica Microsystems, US) through a noncontact approach (Figure 4). The fabric thickness was measured by using a dial thickness gauge (Model H, PEACOCK OZAKI MFG. CO.

LTD, Japan) with a measured force that was less than 1.8 N and an accuracy of 0.01 mm. According to Archimedes' principle, a substance submerged in a liquid displaces a volume of liquid equal to its volume.[49, 50] Thus, the volume of the fabric was calculated by measuring the volume of the displaced water. Each fabric was tested 3 times and the mean value obtained from 15 tests was used.

(a)   (b)
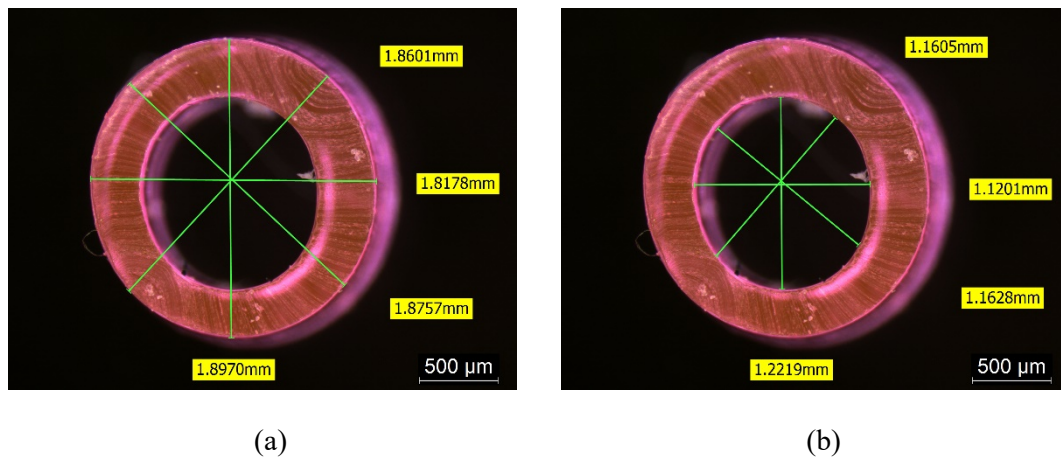
Figure 4. Microscopic view of the P1 tube measured at (a) the outer diameter; (b) the inner diameter

Volume of fabric

The volume of the inlaid knitted fabric was used to calculate its net buoyant force.[48] The samples were immersed in water for 24 hours in accordance with ISO Standard 12402-9:2006.[51] The samples were then taken out and laid flat on a metal rack (in the absence of a ventilating fan) until the interval between every two drops of water was

greater than 30 s. It was assumed that the spaces in the fabric samples were completely filled with water after immersion for 24 hours, and that the excess water was removed by laying the fabric samples flat on the rack. The weight of the wet samples was measured by using an electric balance with a resolution of 0.001 g and the mean value of the weight of each sample obtained from the 15 measurements was recorded (as W_f, in grams).

The weight of the container when completely filled with water was measured and recorded (as W_1, in grams). The wet sample was submerged in the container by pressing down on the glass lid until there were no air bubbles, and the water was then allowed to drain from the container (Figure 5). After draining, a dry cloth was used to dry the outer wall of the container. The weight of the whole system was measured using an electric balance and recorded (as W_2, in grams). The test was repeated three times for each sample.

The mass of water displaced by the sample in the container is

$$M_w = W_1 - (W_2 - W_f), \qquad (1)$$

where M_w is the mass of the water displaced by the sample, W_1 is the weight of the container when filled with water, W_2 is the weight of the container with the water and sample and W_f is the mean wet mass of the sample. This was then converted into the volumetric unit by the following equation.

$$V_f = \frac{M_w}{1\,000\,000}, \qquad (2)$$

where M_w is the mass of the water displaced by the sample (g) and V_f is the volume of

the sample (m³).

Net buoyant force of fabric samples

Following Archimedes' principle, the net buoyant force of the samples is calculated as

follows: [52]

$$F_{net} = \rho_f \, V_f \, g - mg \qquad (3)$$

where F_{net} is the net buoyant force (N), ρ_f is the density of the water ($\rho_f = 1000$ kg/m³),

V_f is the volume of the sample in m³, g is the Earth's standard gravity ($g = 9.807$ m/s²)

and m is the mass of the sample (kg). The mass of the sample can be measured by using

an electric balance.
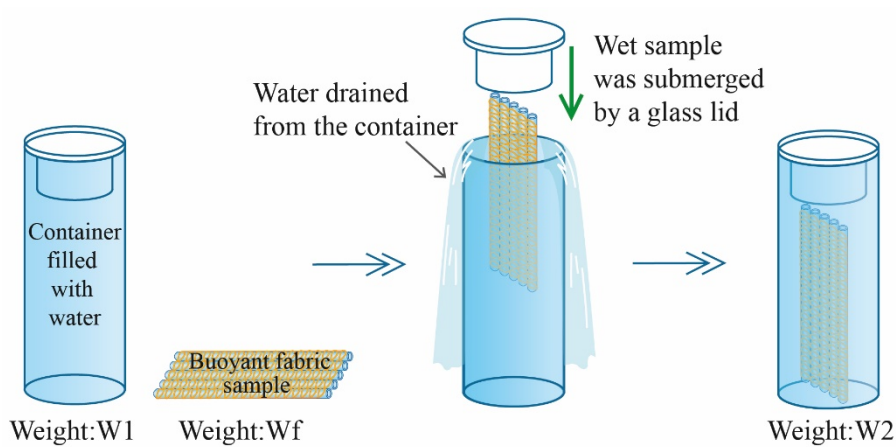
Figure 5. Method for measuring fabric volume

16

Compression and tensile

The linearity of compression, LC, the compression energy, WC (N.m/m²) and the compression resilience, RC (%) were measured in a compression test using an automatic compression tester (KESFB3-AUTO-A, KATO TECH CO., LTD., Japan). A testing speed of 0.040 mm/sec, compression area of 2 cm^2 and maximum load of 50 g/cm^2 were used. Each fabric sample was tested once on three different regions of the sample. The mean value obtained from the 3 tests was used. The tensile properties of the samples in both the wale and course directions were measured with an Instron 4411 tensile tester (Instron CO., LTD., USA). An elongation rate of 100 mm/min and spacing of 5 cm between line clamps were used. As the aim is to replace the foam compartment in conventional buoyant swimwear with the buoyant fabric, a fabric strain at 20% was used and compared instead of using the breaking strain. The maximum load (N) and the energy at the maximum load (J) required to elongate the fabric by 20% of its original length were measured. Three samples were tested for each fabric type and each sample was tested once in both wale and course directions. The samples were conditioned for 24 hours at 20 ± 1℃ and 65% ± 5% relative humidity before measurement and all experiments were carried out at this standard laboratory conditions.

Statistical Analysis

The data from the experiment were analysed using SPSS 23 (IBM Corp., Armonk, New York). MANOVA was used to examine the mean differences among the levels of three different independent variables: (1) inlaid material, (2) yarn and (3) knitted structure on three dependent variables (net buoyant force, compression, and tensile properties). Prior to implementing the MANOVA, the data were evaluated to ensure that the assumptions for the multivariate tests were met. Measurements of skewness and kurtosis, histograms and normal Q-Q plots were examined for the dependent variables (net buoyant force; LC, WC and RC from the compression test; maximum load and energy at maximum load from the tensile test). Observations of these measurements and plots show a normal distribution for the levels of LC, WC and RC. On the other hand, net buoyant force, maximum load and energy at maximum load in both directions were considerably positively skewed. Thus, a logarithm transformation was applied for the net buoyant force and a square root transformation was applied for the maximum load and the energy at the maximum load in both directions. An evaluation of the newly transformed distributions indicated that they were close to a normal curve. The significance level of the statistical analysis was set at 0.05.

Results and discussion

The experimental results are given in Table 6 and plotted in Figures 6 to 10. The coefficients of variation (CV%) for repeated tests are generally less than 5%. The CV% of the net buoyant force of PV2, SI2 and SIF1 is higher than 5% due to their low buoyancy. Only the independent variables with a significant relationship with the dependent variables in MANOVA are shown in Table 7. The results of the mechanical properties are given in Appendixes A and B.

Table 6. Physical properties and net buoyant force of the knitted fabrics

Sample code	Fabric weight (g/m²)	Thickness (mm)	Wale density (Wale/cm)	Course density (Course/cm)	Net buoyant force (N) Mean	SD
PV1	708.94	2.42	3.04	4.51	0.03	0.00
PV2	1083.10	2.90	2.97	4.44	0.04	0.01
SI1	346.26	1.50	2.99	4.80	0.06	0.00
SI2	1023.75	2.38	2.96	4.69	0.03	0.00
SI3	1299.11	3.15	2.95	4.16	0.10	0.00
PE1	315.15	2.31	3.13	4.97	0.05	0.00
PE2	412.23	2.90	2.90	4.29	0.14	0.00
PE3	511.04	4.29	2.91	3.84	0.29	0.02
PE4	720.29	6.54	2.87	4.06	0.41	0.03
EPE1	131.39	4.86	2.69	2.33	0.87	0.01
EPE2	142.82	5.70	2.70	2.16	1.11	0.04
EPE3	118.66	5.73	2.70	2.09	1.40	0.01
SIF1	333.04	1.41	3.48	4.73	0.02	0.00
SIF2	793.70	2.57	2.95	4.27	0.08	0.00
SIF3	1362.61	3.21	2.96	4.04	0.08	0.00
SIF4	2439.99	4.22	2.98	3.39	0.08	0.00
EPEm1	132.46	4.94	2.71	2.11	0.87	0.01
EPEm2	144.59	5.66	2.72	2.00	1.11	0.02
EPEm3	120.73	5.92	2.75	1.93	1.36	0.03
EPEn1	128.70	4.78	2.65	2.59	0.82	0.01
EPEn2	150.30	5.50	2.70	2.52	1.00	0.01
EPEn3	128.13	5.51	2.67	2.59	1.18	0.01
EPEnH1	141.79	4.90	2.63	2.53	0.92	0.02
EPEnH2	171.01	5.90	2.68	2.56	1.13	0.02
EPEnH3	149.16	5.97	2.72	2.58	1.23	0.03
Ch	72.01	0.07	3.20	2.43	0.00	0.00
Cm	86.63	0.08	3.72	2.02	0.00	0.00
Cn	54.87	0.06	2.77	2.79	0.00	0.00
CnH	98.05	0.08	2.29	4.67	0.00	0.00

Table 7. MANOVA Summary Table

Source [h]	Properties	Dependent variable	Type Ⅲ Sum of Squares	df	Mean Square	F	Sig.
Inlaid material [f]	Buoyancy	Net buoyant force [a]	10.17	4	2.54	64.65	0.00
	Compression	LC	0.14	4	0.03	3.36	0.01
		RC	2271.45	4	567.86	13.72	0.00
	Tensile	Maximum load (Wale direction) [b]	79.77	4	19.94	4.98	0.00
		Energy at maximum load (Wale direction) [c]	0.32	4	0.08	4.17	0.01
		Maximum load (Course direction) [d]	810.87	4	202.72	59.09	0.00
		Energy at maximum load (Course direction) [e]	5.92	4	1.48	57.87	0.00
Knitted structure [g]	Compression	WC	2.34	2	1.17	10.25	0.00
	Tensile	Maximum load (Wale direction) [b]	82.55	2	41.28	10.30	0.00
		Energy at maximum load (Wale direction) [c]	0.43	2	0.21	11.25	0.00

Note: all coefficients are rounded to the last two decimals.

[a] Logarithm of net buoyant force

[b] Square root of maximum load (Wale direction)

[c] Square root of energy at maximum load (Wale direction)

[d] Square root of maximum load (Course direction)

^{e} Square root of energy at maximum load (Course direction)

^{f} Pillai's trace= 2.32, $F_{(df=32, 248)}$ =10.75, $p<.001$, $\eta^2=.58$

^{g} Pillai's trace= .71, $F_{(df=16,120)}$ =4.13, $p<.001$, $\eta^2=.36$

^{h} No significant difference found between yarns (Pillai's trace= .13, $F_{(df=8,\ 59)}$ =1.07, $p>.05$, $\eta^2=.13$)
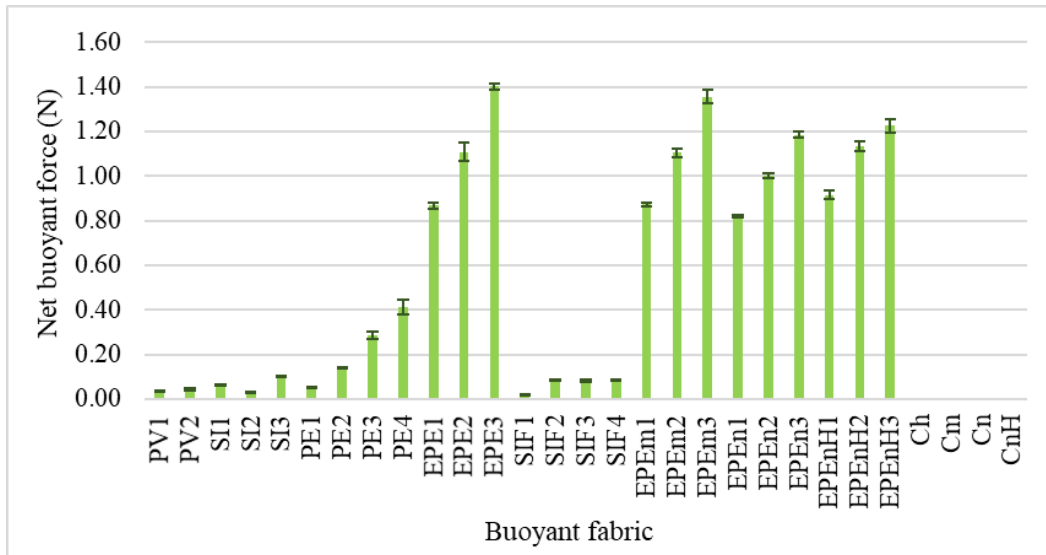
Figure 6. The net buoyant force of the buoyant fabrics and the control fabrics
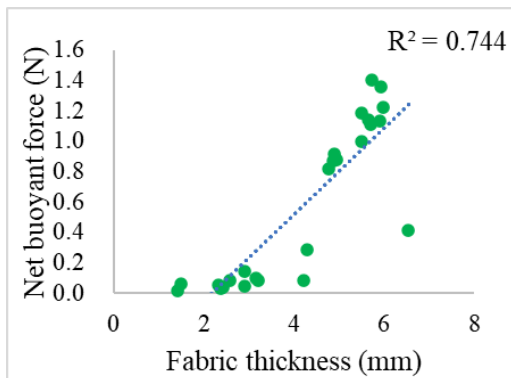
Figure 7. Comparison of the net buoyant force of inlaid knitted fabrics and thickness

22
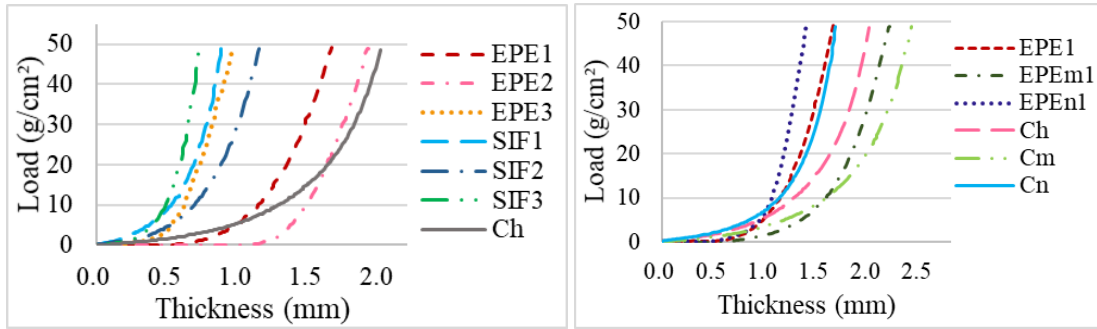
(a)   (b)

Figure 8. Compression behaviours of fabrics with various (a) inlaid materials and (b) knitted structures
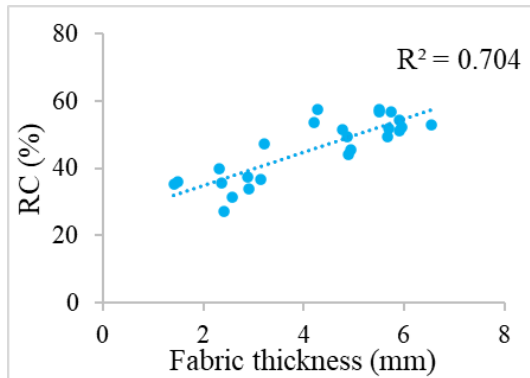
Figure 9. RC vs fabric thickness
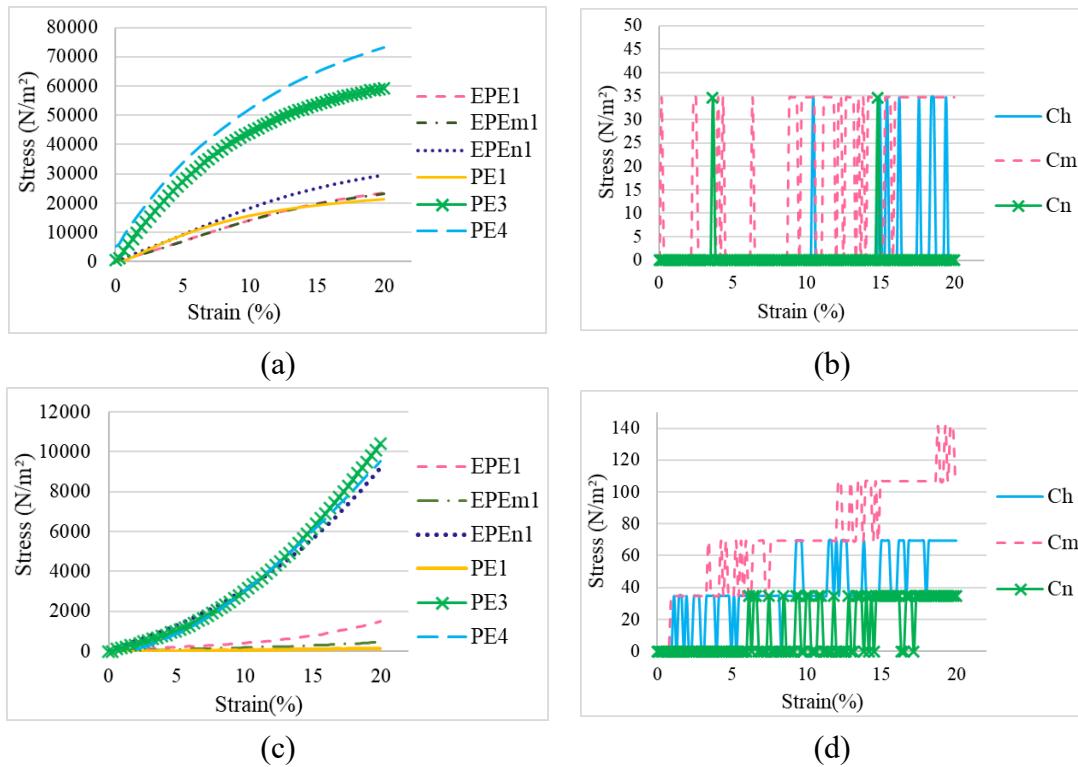
Figure 10. Stress-strain curves of tensile properties in course direction: (a) inlaid fabrics; (b) control fabrics and wale direction for (c) inlaid fabrics and (d) control fabrics

The results of the MANOVA show an overall significant difference between the inlaid material (Pillai's trace= 2.32, $F_{(32,248)}$ =10.75, $p<.001$) and knitted structure (Pillai's trace= .71, $F_{(16,120)}$ =4.13, $p<.001$) on the buoyancy and mechanical properties. However, no significant difference was found between the different types of yarns (Pillai's trace= .13, $F_{(8,59)}$ =1.07, $p>.05$) (Table 7). The inlaid material accounts for 58 percent of the variance in the overall buoyancy and mechanical properties (η^2=.581) and knitted structure accounted for 36 percent (η^2=.355). This implies that the variances

in the buoyancy and mechanical properties of the fabrics are mainly due to the inlaid material.

The results of the post hoc between-subjects comparison indicate that five types of inlaid material are significantly different in terms of the net buoyant force (F=64.65, $p<.001$, $\eta^2=.797$), LC (F=3.36, $p<.02$, $\eta^2=.169$), RC (F=13.72, $p<.001$, $\eta^2=.454$), maximum load of tensile elongation (wale direction: F=4.98, $p<.01$, $\eta^2=.232$; course direction: F=59.09, $p<.001$, $\eta^2=.782$) and energy at maximum load (wale direction: F=4.17, $p<.02$, $\eta^2=.202$; course direction: F=57.87, $p<.001$, $\eta^2=.778$). Besides, the knitted structure shows a significant difference only for WC (F=10.25, $p<.001$, $\eta^2=.237$), maximum load (F=10.30, $p<.001$, $\eta^2=.238$) and energy at maximum load when elongated in the wale direction (F=11.25, $p<.001$, $\eta^2=.254$).

Net Buoyant Force

The inlaid material accounts for 80 percent of the variance in the overall buoyancy ($\eta^2=.797$). This confirms that the fabric's buoyant force was mainly affected by the inlaid material. The inlaid knitted fabrics also demonstrated a higher net buoyant force than all of the control fabrics, as shown in Figure 6. Following Archimedes' principle, the net buoyant force can be calculated by using the weight and volume of the sample.[52] As equation 3 shows, the higher net buoyant force is a function of a smaller fabric

weight and of greater volume of fabric sample. Therefore, the net buoyant force of the inlaid knitted fabrics increases with fabric thickness (Figure 7). When EPEm1, EPEm2 and EPEm3 were compared, the net buoyant force was found to increase with the fabric's thickness and the outer diameter of the inlaid material, as shown in Tables 5 and 6, indicating that the fabric thickness was mainly affected by the diameter of the inlaid material. The air bubbles inside the foam rods increased with the diameter of the inlaid material and resulted in a higher net buoyant force. However, SIF2, SIF3 and SIF4 have the same net buoyant force even with increased diameter of the inlaid material. This implies that silicone foam with a larger diameter does not increase the volume of air and provides the same amount of buoyancy.

When EPE3, EPEm3 and EPEn3 were compared, EPEn3 in the 1x1 rib structure was found to have the lowest net buoyant force (Figure 6). The area of space for the foam rod to be laid-in was lowest in the 1x1 rib structure, as the highest course density appeared in this knitted structure (Table 6). The inlaid material was then squeezed between the loops and the air inside the foam was reduced, which resulted in EPEn3 exhibiting the lowest net buoyant force among the three fabrics. Although EPEm3 had a lower course density than EPE3, their net buoyant force was similar. There was more space between the front and back loops in the full milano than in the half milano, but this did not increase the net buoyant force of the fabric. As no squeezing of the inlaid

material occurred when it was knitted with both half milano (EPE3) and full milano (EPEm3), a similar net buoyant force resulted.

Compression properties

LC can be denoted by the linearity of the curve plotted of the compression vs. thickness.[53] WC is the amount of energy required to compress a fabric.[54] RC indicates the recoverability of a fabric after the compression force is removed.[55] When the RC value approaches 100%, this denotes better resilience. The results of the MANOVA indicates that the LC and RC of the fabric with inlaid materials significantly differ with various inlaid materials whereas the WC significantly differs with the knitted structure (Table 7). However, only 17% of the variance in LC (η^2=.169) and 45% of the variance in the RC (η^2=.454) are accounted for by the inlaid material and 24% of the variance in the WC is accounted for by the knitted structure (η^2=.237).

SIF3 (inlaid with silicone foam) shows a more sensitive response to the compression force as can be observed by a steeper curve of the compression load vs. thickness (larger slope) in Figure 8a. EPE2 is more easily compressible than EPE1 when the diameter of the inlays is increased. However, EPE3 is barely compressible when the diameter of the inlays is further increased. This is because the fabric becomes tighter when a foam rods used have a larger diameter. As shown in Figure 8b, the

27

compression curve of the knitted fabric samples with inlays, EPE1, EPEm1 and EPEn1, and the control fabric samples, Ch, Cm and Cn, have a similar shape. This is in agreement with the MANOVA result in which there is no significant difference in the LC with knitted structure. When comparing the inlaid and control fabric samples with the same knitted structure at 30 g/cm² load, the control fabrics might easily compress as it has higher thickness values at an equivalent load. This shows that the fabric samples become less compressible with the incorporation of inlays.

For single jersey knitted fabric, WC and RC increased when the fabric had a lower stitch density.[56] Unlike for the single jersey knitted fabric, the RC of the inlaid knitted fabrics increased with the fabric's thickness ($R^2=.70$), but this was not related to stitch density (Figure 9). The effect of the knitting yarn on the fabric's thickness was negligible when compared with that of the inlaid material, and thus the increase in the fabric's thickness was mainly due to the increase in the outer diameter of the inlaid material. With an increase in the diameter of the inlaid material, the fabric with a higher RC value indicates that it has better recoverability.

Tensile properties

Maximum load (N) in a 20% elongation is the force needed to elongate the fabric by 20% from its original dimension. A higher maximum load indicates that the fabric is

28

stronger. Higher energy at the maximum load (J) means that the fabric is tougher in terms of breakage at a 20% elongation. Liu et al. showed that the length-wise and width-wise elongation properties of the fabric are significantly affected by the inlaid stitch used.[45] Unlike their study, the inlaid material in this study accounts for 78 percent of the variance at the maximum load (η^2=.782) and energy at maximum load (η^2=.778) when the fabric is elongated in the course direction. For elongation in the wale direction, the inlaid material and knitted structure account for less than 30% of the variance at maximum load (inlaid material: η^2=.232; knitted structure: η^2=.238) and energy at maximum load (inlaid material: η^2=.202; knitted structure: η^2=.254).

For the tensile properties in the course direction, the fabric sample with inlaid material that has a larger diameter (PE1 to PE4) show the same trend but with a higher modulus during tensile loading. The fabric has higher strength and is more resistant against breakage in the course direction when the inlaid material has a larger diameter. It also implies that more force is needed to elongate the fabric in the course direction when the diameter of the inlaid material is increased. Besides, the three inlaid fabric samples (EPE1, EPEm1 and EPEn1) and the control fabric samples (Ch, Cm and Cn) with three different knitted structures show a similar trend and slope value (Figures 10a and 10b). This implies that the stiffness of the inlaid knitted and control fabrics in the course direction is not affected by the knitted structure.

EPEn1, PE3 and PE4 show a similar shape in the wale direction for the relationship between stress and strain which implies that fabric with these inlaid materials have a similar stiffness in the wale direction (Figure 10c). Inlaid fabric knitted in 1×1 rib (EPEn1) has the highest stiffness in the wale direction than the half milano (EPE1) and full milano (EPEm1) samples. However, the control fabric sample knitted in full milano has the highest stiffness among the three different structures (Figure 10d) which implies that fabric stiffness in the wale direction is affected by both the knitted structure and the inlaid material. The region that is used to lay in the foam rods is the smallest in the 1×1 rib structure, as the highest course density is found with this knitted structure (Table 6). The loops were tightened by inlaid material which can undertake higher loading during stretching in the wale direction.

The stress of the inlaid knitted fabric at 20% strain is higher than that of the control fabric when elongated in both the wale and course directions (Figure 10). This demonstrates that the inlaid material reinforces the fabric in the wale and course directions. As shown in Figures 10a and 10c, the stress of each inlaid fabric sample at 20% strain in the course direction is higher than that of the sample in the wale direction. This implies that the inlaid fabric is significantly reinforced in the course direction and less deformable due to the inlaid material.[42]

Conclusion

The aim of this study is to develop buoyant inlaid knitted fabrics for buoyant swimwear applications. The mean differences among the inlaid material, yarn and knitted structure on net buoyant force, compression, and tensile properties have been examined. The results reveal that the net buoyant force and mechanical properties of the fabric are significantly different depending on the inlaid material and knitted structure but not yarn. The variance in mechanical properties is mainly due to the inlaid material and the net buoyant force is significantly different with only inlaid material. The net buoyant force is found to increase with fabric thickness and the outer diameter of the inlaid material.

In terms of the compression properties, LC and RC are significantly different with the inlaid material whereas WC shows a significant difference with the knitted structure. The inlaid fabric is less compressible than the control fabric with the same knitted structure. The inlaid fabric which has inlaid material with a larger outer diameter shows a higher RC which indicates better recoverability. The tensile properties of the inlaid fabric in the course direction are significantly reinforced by the inlaid material in which a larger diameter of the inlays contributes to a stronger fabric that resists breakage. In the wale direction, the knitted structure and inlaid material show significant differences in the maximum load and energy at maximum load. However,

they only account for less than 30 percent of the variance. The PP fabric inlaid with

6.36 mm of EPE foam with a half milano structure (EPE3) is a possible candidate for

use in the future development of buoyant swimwear, as it has the greatest buoyancy.

Reference:

1.   Kim S, Lee H, Hong K, et al. Use of three-dimensional technology to construct ergonomic patterns for a well-fitting life jacket of heterogeneous thickness. *Text Res J* 2015; 85: 816-827. DOI: 10.1177/0040517514553874.

2.   YMCA of the USA. *Parents' guide to Y skippers*. Champaign: YMCA of the USA, 1987.

3.   Shank C. *A child's way to water play*. New York: Leisure Press, 1983.

4.   Lee SH. *Buoyant swimsuit*. Patent 15/303739, U.S., 2017.

5.   Ramón JM and Valero A. Use of floating material in swimming. *Apunts Educacio΄ Fι΄sica i Esports* 2018; 2: 48-59. DOI: 10.5672/apunts.2014-0983.es.(2018/2).132.04.

6.   Sahu MM and Bhagoria JL. Augmentation of heat transfer coefficient by using 90[degrees] broken transverse ribs on absorber plate of solar air heater. *Renew Energ* 2005; 30: 2057. DOI: 10.1016/j.renene.2004.10.016.

7.   Gonsalves DJ and Gonsalves KC. *Water sport flotation garment*. Patent 8,591,275, U.S., 2013.

8.   Mann HK. *Item of swimming wear*. Patent 5,452,477, U.S., 1995.

9.   Gómez JH. *Floating swimsuit for learning to swim*. Patent 2014/177731 A1, WIPO (PCT), 2014.

10.   Staver BJ and Vaughn N. *Buoyant swim garment*. Patent 7,438,619 U.S., 2008.

11.   Zheng LY. *Float swimsuit*. Patent CN206303237U, China, 2016.

12.   Grunstein E and Grunstein AC. *Swimwear with buoyant neck support and body panels*. Patent 6,260,199, U.S., 2001.

13.   Meredith JR. *Construction of flotation swimsuits*. Patent 5,459,874, U.S., 1995.

14.   Mitchell JL. *Scuba wet suit with constant buoyancy*. Patent 6,519,774, U.S., 2003.

15.   Li NW, Ho CP, Yick KL, et al. Novel buoyant fabrics created by integrating inlay knitted structure. In: *46th Textile Research Symposium* Susono, Japan, 3-5 September 2018, paper no. 9, pp.9. Japan: The Textile Machinery Society of Japan.

16. Li NW, Ho CP, Yick KL, et al. Development of laid-in knitted fabric for buoyant swimwear. *J Ind Text.* Epub ahead of print January 24, 2020. DOI: 10.1177/1528083719900932.

17. Li NW, Ho CP, Yick KL, et al. New thinking in designing buoyant knitted textiles. In: *6th International Conference on Arts and Humanities*, Kuala Lumpur, Malaysia, 19-20 September 2019, paper no. F2(30), pp.36. Dr. Eldad Tsabary (ed). Sri Lanka: The Institute of Knowledge Management. ISBN 978-955-3605-37-5.

18. Yang Y, Chen L, Naveed T, et al. Influence of fabric structure and finishing pattern on the thermal and moisture management properties of unidirectional water transport knitted polyester fabrics. *Text Res J* 2019; 89: 1983-1996. DOI: 10.1177/0040517518783349.

19. Mark A, Psikuta A, Bauer B, et al. Artificial skin for sweating guarded hotplates and manikins based on weft knitted fabrics. *Text Res J* 2019; 89: 657-672. DOI: 10.1177/0040517517750646.

20. Cho S, Cho G and Kim C. Fabric sound depends on fiber and stitch types in weft knitted fabrics. *Text Res J* 2009; 79: 761-767. DOI: 10.1177/0040517508099915.

21. Dolatabadi MK, Janetzko S and Gries T. Geometrical and mechanical properties of a non-crimp fabric applicable for textile reinforced concrete. *J Text Inst* 2014; 105: 711-716. DOI: 10.1080/00405000.2013.844908.

22. Palani Rajan T, Ramakrishnan G, Sundaresan S, et al. The influence of fabric parameter on low-stress mechanical properties of polyester warp-knitted spacer fabric. *Int J Fash Des Technol Educ* 2017; 10: 37-45. DOI: 10.1080/17543266.2016.1177738.

23. Silich T. Special features of treatment of cotton-polypropylene yarn in knitted fabric production. *Fibre Chem* 2012; 43: 372-375. DOI: 10.1007/s10692-012-9367-y.

24. Maier C and Calafut T. *Polypropylene : The definitive user's guide and databook*. Norwich: Elsevier Science & Technology Books, 1998.

25. Yu S, Zheng Y, Zhou Q, et al. Facile modification of polypropylene hollow fiber microfiltration membranes for nanofiltration. *Desalination* 2012; 298: 49.

26. Xu Z, Liu Z, Song P, et al. Fabrication of super-hydrophobic polypropylene hollow fiber membrane and its application in membrane distillation. *Desalination* 2017; 414: 10-17. DOI: 10.1016/j.desal.2017.03.029.

27. Kalayci E, Yildirim FF, Avinc OO, et al. Textile fibers used in products floating on the water. In: *7th international scientific professional conference: Textile Science and Economy VI* Zrenjanin, Serbia, 25-31 May 2015, pp.85-90. Prof. Vasilije Petrovic (ed). Zrenjanin: University of Novi Sad. ISBN 978-86-7672-255-6.

28. Cai K, Pritikin E, Sandland N, et al. Achieving PVC properties in new medical TPE compounds. *Rubber World* 2011; 244: 18.

29. Lu S, Duan X, Han Y, et al. Silicone rubber/polyvinylpyrrolidone microfibers produced by coaxial electrospinning. *J Appl Polym Sci* 2013; 128: 2273-2276. DOI: 10.1002/app.37848.

30. Kirk DP. *Recreational floatation device with integral cup holder*. Patent 6,790,112, U.S., 2004.

31. Parker TS, Neely G and Parker CP. *Noodle beverage container*. Patent 9,314,119, U.S., 2016.

32. Johnson J, Carlson M and Espelien B. *Foam stabilization for personal flotation device*. Patent 6,986,691, U.S., 2006.

33. Whalley SA. *Locked inlay knit fabrics*. Patent 5,299,435, U.S., 1994.

34. Okuno M and Nakamori T. *Yarn carrier of weft knitting machine*. Patent 7,201,023, U.S., 2007.

35. Leong KH, Ramakrishna S, Huang ZM, et al. The potential of knitting for engineering composites — A review. *Compos Part A* 2000; 31: 197-220. DOI: 10.1016/S1359-835X(99)00067-6.

36. De Araujo M, Fangueiro R and Hu H. Weft-knitted structures for industrial applications. In: Au KF (ed) *Advances in Knitting Technology*. Cambridge: Elsevier Science & Technology, 2011, pp.136-170.

37. Chong HK, Kan CW, Ng SP, et al. Study on the relationship between UV protection and knitted fabric structure. *J Text Eng* 2013; 59: 71-74.

38. Zhang YH, Kan CW and Lam KC. A study on ultraviolet protection properties of 100% cotton knit fabric: effect of fabric structure. *J Text Inst* 2015; 106: 648-654. DOI: 10.1080/00405000.2014.933514.

39. Kurbak A. Models for basic warp knitted fabrics Part I: Chain stitches and their applications on marquisette and weft-inserted warp-knitted fabrics. *Text Res J* 2019; 89: 1863-1885. DOI: 10.1177/0040517518779992.

40. Alpyildiz T, Rochery M, Kurbak A, et al. Stab and cut resistance of knitted structures: a comparative study. *Text Res J* 2011; 81: 205-214. DOI: 10.1177/0040517510383617.

41. Abounaim M, Diestel O, Offmann G, et al. High performance thermoplastic composite from flat knitted multi-layer textile preform using hybrid yarn. *Compos Sci Technol* 2011; 71: 511-519. DOI: 10.1016/j.compscitech.2010.12.029.

42. Balea L, Dusserre G and Bernhart G. Mechanical behaviour of plain-knit reinforced injected composites: Effect of inlay yarns and fibre type. *Compos Part B* 2014; 56: 20-29. DOI: 10.1016/j.compositesb.2013.07.028.

43. Cheng KB, Lee KC, Ueng TH, et al. Electrical and impact properties of the hybrid knitted inlaid fabric reinforced polypropylene composites. *Compos Part A* 2002; 33: 1219-1226. DOI: 10.1016/S1359-835X(02)00076-3.

44. Zhang X and Ma P. Application of knitting structure textiles in medical areas. *Autex Res J* 2018; 18: 181-191. DOI: 10.1515/aut-2017-0019.

45. Liu R, Lao TT and Wang SX. Impact of weft laid-in structural knitting design on fabric tension behavior and interfacial pressure performance of circular knits. *J Eng Fibers Fabr* 2013; 8: 96-107. DOI: 10.1177/155892501300800404.

46. Siddique Hafiz F, Mazari Adnan A, Havelka A, et al. Development of V-shaped compression socks on conventional socks knitting machine. *Autex Res J* 2018; 18: 377-384. DOI: 10.1515/aut-2018-0014.

47. Alisauskiene D, Mikucioniene D and Milasiute L. Influence of inlay-yarn properties and insertion density on the compression properties of knitted orthopaedic supports. *Fibres Text East Eur* 2013; 21: 74-78.

48. Li NW, Ho CP, Yick KL, et al. Comparison of test methods for measuring the net buoyant force of buoyant materials. *Res J Text Apparel* 2020; 24: 147-161.

49. Kiriktas H, Sahin M, Eslek S, et al. A New Approach to Determine the Density of Liquids and Solids without Measuring Mass and Volume: Introducing the "Solidensimeter". *Phys Educ* 2018; 53: 1-6. DOI: 10.1088/1361-6552/aaa91e.

50. Van Daal M. Buoyancy and density. *Int Cranes Spec Trans* 2015; 24: 41-42.

51. ISO 12402-9:2006. Personal flotation devices - Part 9: Test methods.

52. Picelli R, Van Dijk R, Vicente WM, et al. Topology optimization for submerged buoyant structures. *Eng Optim* 2017; 49: 1-21. DOI: 10.1080/0305215X.2016.1164147.

53. Zhang Q and Kan CW. Property comparison of woollen fabrics with fusible and printable interlinings. *Fibers Polym* 2018; 19: 987-996. DOI: 10.1007/s12221-018-8167-2.

54. Xiao X, Hua T, Wang J, et al. Transfer and mechanical behavior of three-dimensional honeycomb fabric. *Text Res J* 2015; 85: 1281-1292. DOI: 10.1177/0040517514561921.

55. Zhang Q, Kan CW and Chan CK. Relationship between physical and low-stress mechanical properties to fabric hand of woollen fabric with fusible interlinings. *Fibers Polym* 2018; 19: 230-237. DOI: 10.1007/s12221-018-7464-5.

56. Kane CD, Patil UJ and Sudhakar P. Studies on the Influence of Knit Structure and Stitch Length on Ring and Compact Yarn Single Jersey Fabric Properties. *Text Res J* 2007; 77: 572-582. DOI: 10.1177/0040517507078023.

Appendix A. Compression properties of the knitted fabrics

Fabric code	LC		WC (N.m/m²)		RC (%)	
	Mean	SD	Mean	SD	Mean	SD
PV1	0.50	0.18	1.76	0.37	27.23	6.10
PV2	0.47	0.06	1.26	0.33	33.98	1.29
SI1	0.51	0.05	1.63	0.22	35.94	1.55
SI2	0.52	0.07	1.24	0.12	35.64	1.19
SI3	0.46	0.01	0.62	0.09	36.74	1.97
PE1	0.47	0.02	1.45	0.22	39.85	2.90
PE2	0.46	0.04	1.08	0.27	37.39	3.29
PE3	0.42	0.07	1.22	0.44	57.55	10.46
PE4	0.76	0.09	1.37	0.31	52.90	0.27
EPE1	0.61	0.07	1.66	0.08	49.32	0.80
EPE2	0.71	0.10	1.39	0.05	51.74	1.69
EPE3	0.67	0.06	1.15	0.08	56.88	1.13
SIF1	0.54	0.05	1.08	0.04	35.11	1.17
SIF2	0.57	0.04	1.46	0.32	31.48	1.74
SIF3	0.52	0.07	0.75	0.02	47.40	1.09
SIF4	0.46	0.02	1.58	0.23	53.66	2.76
EPEm1	0.53	0.03	1.99	0.06	45.53	0.70
EPEm2	0.60	0.02	1.87	0.05	49.34	0.71
EPEm3	0.64	0.02	2.08	0.12	51.15	0.46
EPEn1	0.65	0.03	1.27	0.02	51.40	1.26
EPEn2	0.78	0.07	1.13	0.09	56.79	1.19
EPEn3	0.59	0.09	1.51	0.07	57.57	2.18
EPEnH1	0.48	0.10	1.29	0.04	43.89	3.33
EPEnH2	0.67	0.05	0.79	0.03	54.31	0.73
EPEnH3	0.75	0.02	1.78	0.20	52.22	1.73
Ch	0.49	0.02	2.16	0.05	35.87	0.90
Cm	0.48	0.01	2.45	0.06	36.65	0.14
Cn	0.44	0.01	1.80	0.13	33.89	0.27
CnH	0.21	0.03	3.16	0.50	28.59	0.58

Appendix B. Tensile properties of the knitted fabrics

Fabric code	20% Elongation in course direction				20% Elongation in wale direction			
	Maximum load (N)		Energy at maximum Load (J)		Maximum load (N)		Energy at Maximum Load (J)	
	Mean	SD	Mean	SD	Mean	SD	Mean	SD
PV1	273.87	15.08	1.97	0.11	0.80	0.13	0.00	0.00
PV2	227.38	15.85	1.39	0.11	1.65	0.34	0.01	0.00
SI1	24.56	2.08	0.14	0.01	0.71	0.08	0.00	0.00
SI2	57.71	3.95	0.38	0.02	1.43	0.28	0.01	0.00
SI3	80.18	4.43	0.52	0.03	5.14	1.73	0.02	0.01
PE1	78.61	1.32	0.51	0.03	0.67	0.00	0.00	0.00
PE2	152.66	9.97	1.07	0.08	3.84	1.02	0.02	0.00
PE3	228.77	4.63	1.58	0.07	47.73	5.91	0.18	0.03
PE4	282.95	5.72	1.93	0.06	44.52	6.49	0.19	0.04
EPE1	91.45	4.11	0.53	0.03	5.64	0.70	0.02	0.00
EPE2	102.75	1.24	0.57	0.01	32.39	1.41	0.13	0.01
EPE3	60.80	0.94	0.29	0.01	37.58	4.90	0.16	0.02
SIF1	3.39	0.62	0.02	0.00	0.67	0.00	0.00	0.00
SIF2	9.35	0.31	0.05	0.00	1.11	0.16	0.00	0.00
SIF3	21.87	1.41	0.12	0.01	9.44	3.82	0.03	0.01
SIF4	46.75	2.65	0.27	0.01	74.62	20.19	0.39	0.07
EPEm1	85.14	2.64	0.50	0.02	1.69	0.31	0.01	0.00
EPEm2	91.27	3.14	0.46	0.02	11.85	4.95	0.04	0.02
EPEm3	44.34	3.76	0.21	0.02	15.84	2.89	0.06	0.01
EPEn1	111.27	2.38	0.65	0.01	41.38	5.17	0.17	0.03
EPEn2	115.83	2.15	0.63	0.01	62.23	1.93	0.29	0.01
EPEn3	70.46	1.17	0.35	0.00	50.69	0.89	0.24	0.01
EPEnH1	103.93	3.76	0.60	0.02	21.89	2.45	0.08	0.01
EPEnH2	123.75	1.08	0.66	0.02	46.44	0.19	0.22	0.00
EPEnH3	70.29	3.35	0.34	0.02	41.81	2.32	0.20	0.01
Ch	0.03	0.04	6.00×10^{-5}	0.00	0.28	0.03	1.35×10^{-3}	0.00
Cm	0.13	0.00	5.60×10^{-4}	0.00	0.44	0.08	2.13×10^{-3}	0.00
Cn	0.00	0.00	4.00×10^{-5}	0.00	0.13	0.00	5.10×10^{-4}	0.00
CnH	0.07	0.05	3.50×10^{-4}	0.00	0.16	0.09	1.08×10^{-3}	0.00